Available online at www.sciencedirect.com
SCIENCE DIRECT®
Mechanism and Machine Theory 39 (2004) 1207–1221
Mechanism and Machine Theory
www.elsevier.com/locate/mechmt

Kinematic analysis of geared mechanisms using the concept of kinematic fractionation

Chia-Pin Liu, Dar-Zen Chen *, Yu-Tsung Chang

Department of Mechanical Engineering, National Taiwan University, Taipei 10660, Taiwan

Received 14 May 2002; received in revised form 3 May 2004; accepted 28 May 2004

Abstract

A systematic approach to the determination of kinematic relations between input(s) and output(s) in geared mechanisms is presented based on the concept of kinematic fractionation. It is shown that kinematic unit (KU) can be viewed as functional building block of geared mechanisms, and kinematic propagation path from input to output can be determined systematically according to the interface among KUs. The local gain between the local input and output of each KU can be systematically formulated. Along the propagating path connecting input and output, global kinematic relation can then be evaluated by collecting local gains of KUs. It is believed that this unit-by-unit evaluation procedure provides a better insight of the effects of each KU on the interactions among input(s) and output(s). An epicyclic-type automatic transmission mechanism is used to illustrate the procedure.

1. Introduction

Geared mechanisms have been used widely as power transmission and force amplification devices in machines and vehicles. The input power is transmitted to output through a path composed of meshing gear pairs and corresponding carriers. Through kinematic analysis, dependent relations among input(s) and output(s) of the mechanism are evaluated.

* Corresponding author. Fax: +886 2363 1755.
E-mail address: dzchen@ccms.ntu.edu.tw (D.-Z. Chen).

0094-114X/$ - see front matter © 2004 Elsevier Ltd. All rights reserved.
doi:10.1016/j.mechmachtheory.2004.05.010

Many research efforts had been devoted to develop efficient approaches to the kinematic analysis of geared mechanisms. Some basic methods, such as the tabular method and formula method have been widely known and elaborated in the textbooks [1–3]. Although these methods provide basic skills to investigate the kinematic relations among input(s) and output(s), it can be laborious as these procedures are applied to complex gear trains. Based on the application of graph theory [4], the concept of fundamental circuit was applied to the kinematic analysis of gear trains [5,6]. However, the determination of the kinematic relations needs to solve a set of linear equations simultaneously. The mathematical manipulation cannot provide much insight into the kinematic structure of the mechanism. Chatterjee and Tsai [7] established the concept of fundamental geared entity (FGE) for automatic transmission mechanisms and applied the concept to associated speed ratio analysis and power loss analysis [8]. However, the concept of FGE can only be applied to reverted type epicyclic gear trains and is specialized in determining kinematic relations among coaxial links. Chen and Shiue [9] showed that a geared robotic mechanism can be regarded as a combination of input units and transmission units. Chen [10] verified the forward and backward gains of each unit and proposed a unit-by-unit evaluation procedure for the kinematic analysis of geared robotic mechanisms. Although this approach is straightforward and provides clear kinematic insight in the torque transmission, it is restricted to geared robotic mechanisms.

Based on the concept of kinematic fractionation developed by Liu and Chen [11], a method to determine the kinematic propagation path from input to output links in geared mechanisms will be established in this paper. It will be shown that a geared mechanism can be regarded as a combination of kinematic units (KUs). The connection among KUs reveals the kinematic propagating path in the mechanism, and the kinematic relationship between input and output links can be formulated efficiently by combining local gain of each KU along the path. The kinematic modules in turn serve as an efficient tool to determine complicated kinematic relations among input(s) and output(s). It is believed that the concept of kinematic fractionation can provide lucid perspective to determine kinematic relations in a geared mechanism.

2. Concept of kinematic fractionation

In the graph representation of geared mechanisms, links are represented by vertices, gear pairs by heavy edges, turning pairs by thin edges, and each thin edge is labeled according to the associated axis location. Liu and Chen [11] defined the KU as a basic kinematic structure in geared mechanisms. Each KU is composed of a carrier and all the gears on it. A graph-based procedure to identify the KUs in a geared mechanism [12] is briefly described as follows with an illustration on the graph representation of epicyclic gear train (EGT) in Fig. 1:

Step 1: Construct the displacement graph [4]. Fig. 1(b) shows the displacement graph of Fig. 1(a).

Step 2: Separate the displacement graph into sub-graph(s) each with only one carrier label. Fig. 1(c) shows the separated displacement graph of Fig. 1(b).

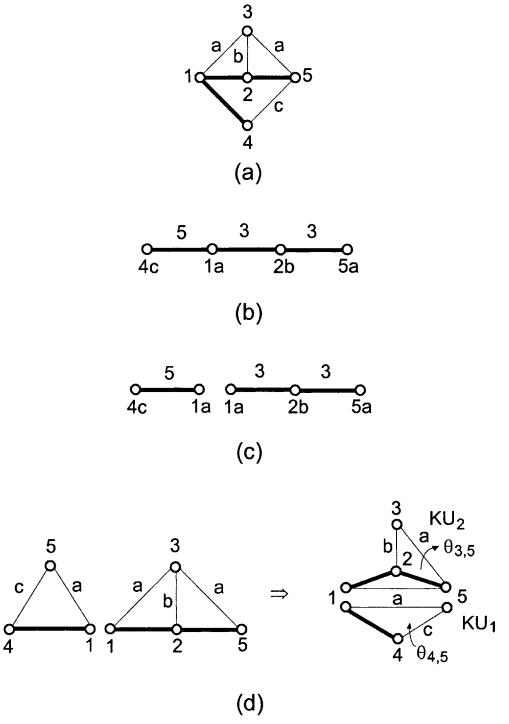

Fig. 1. Graph representation of 5-link EGT. (a) Graph representation, (b) displacement graph, (c) separated displacement graph, (d) resultant KUs.

Step 3: Add a carrier vertex to each segment of the separated displacement graph and connect the gear–carrier pairs by thin edges. Each thin edge is then labeled with axis orientations. The example result is shown to the left of Fig. 1(d) in which vertices 1 and 5 are common to both sub-graphs.

Step 4: In each sub-graph obtained in *Step 3*, identify the vertices which are shared as common links, and connect these vertices with a thin edge. Each resultant sub-graph is referred to as a KU. Since vertices 1 and 5 in Fig. 1(d) are coaxial, a thin edge can be formed by coaxial re-arrangement without changing kinematic characteristics of the mechanism [13]. Fig. 1(d) shows the KUs of Fig. 1(a) on the right hand side.

By applying above procedure, EGTs with 1-dof 5-link enumerated by Freudenstein [4] and Tsai [14] and EGTs with 2-dof 6-link enumerated by Tsai and Lin [13] can be fractionated systematically. Fig. 2(a) shows 1-dof 5-link EGTs with only one KU, and Fig. 2(b) shows EGTs with multiple KUs. Fig. 3 shows 2-dof 6-link EGTs with 3 KUs. In Figs. 2 and 3, it can be seen that there are 10 distinct KUs can be identified and shown in Table 1. In Table 1, each KU is labeled with Kn-# where n is the number of links and # is the serial number.

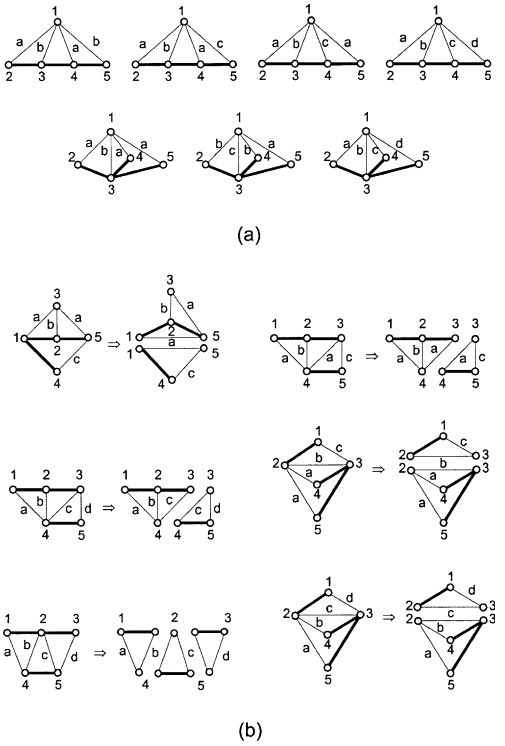

Fig. 2. Kinematic fractionation of 1-dof 5-link EGTs. (a) EGTs with one KU, (b) EGTs with more than one KU.

3. Internal conversion

3.1. Admissible internal conversion modes

Liu and Chen [11] showed that each KU can be regarded as a 1-dof sub-mechanism in the geared mechanism since the kinematic relations among links can be determined by a single input. In each KU, motion is initiated by the local input, which is either a contained input or the common linkage connecting to the preceding KU(s). The local input of a KU is then modulated, and transmitted to the local output, which is either the global output or the common linkage connecting to the succeeding KU(s). This process of transforming and transmitting from local input to local output within a KU is referred to as the internal conversion.

Both the local input and output in the KU can be expressed as the relative angular displacement between a turning pair, which is corresponding to a thin edge in graph representation. According to the types of adjacent vertices, thin edges in a KU can be classified into two different types:

(1) gear–carrier (g–c) type: One end of the thin edge is a gear vertex, and the other end is a carrier vertex. A g–c type thin edge is denoted by a thin line as shown in Table 1.
(2) gear–gear (g–g) type: Both ends of the thin edge are gear vertices. A g–g type thin edge is distinguished from the g–c type thin edges by a double line representation.

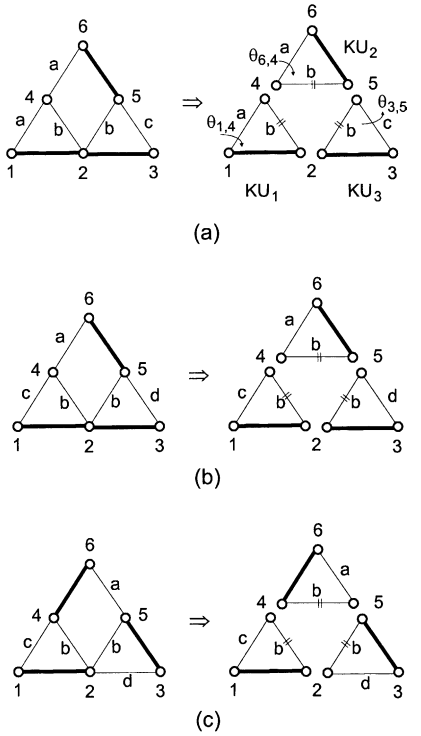

Fig. 3. Kinematic fractionation of 2-dof 6-link EGTs.

Table 1
Local gains for up-to-5 link KUs with g–c vs. g–c internal conversion mode

KUs	
	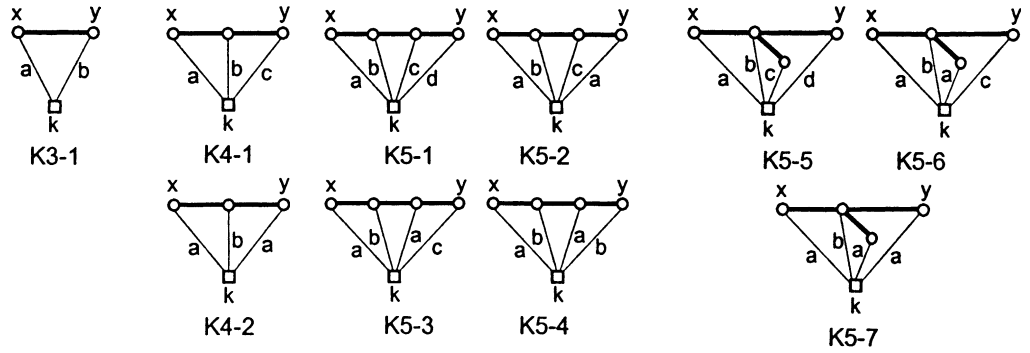
	K3-1 K4-1 K5-1 K5-2 K5-5 K5-6 K4-2 K5-3 K5-4 K5-7
Local gain	$G(y,k;x,k)=\frac{\theta_{y,k}}{\theta_{x,k}}=E_{x,y}$

Note that a g–g type thin edge in a KU can be formed by coaxial re-arrangement as the thin edges connecting each of the two gear vertices and the carrier have the same axis label. As a g–g type thin edge is added to a KU, one of the coaxial g–c type thin edges should be deleted.

The KUs, which can include g–g type thin edge(s), are collected as shown in Tables 2 and 3. Each KU in Table 2 is labeled as Kn-#S which indicates that the KU is originated from Kn-# with single g–g type thin edge. Similarly, each KU in Table 3 is labeled as Kn-# D which indicates that the KU is originated from Kn-# with double g–g type thin edges. Note that one of the coaxial g–c type thin edges of KUs in Table 2 and two of the coaxial g–c type thin edges of KUs in Table 3 can be removed arbitrarily.

Among these thin edges, a KU can have at least one of the following three internal conversion modes:

Case 1. g–c vs. g–c type: The internal conversion is between two g–c type thin edges. Both the local input and output of the KU are located on g–c type thin edges. For KUs with up to five links, this internal conversion mode can take place between any two thin edges in Table 1.

Case 2. g–c vs. g–g type: The internal conversion is between a g–c type thin edge and a g–g type thin edge. The local input and output of the KU are located on different types of thin edges. For KUs with up to five links, this internal conversion mode can take place between the g–g type thin edge and any one of the g–c type thin edges in Table 2.

Case 3. g–g vs. g–g type: The internal conversion is between two g–g type thin edges. Both the local input and output of the KU are located on g–g type thin edges. For KUs with up to five links, this internal conversion mode can take place between the two g–g type thin edges in Table 3.

Table 2
Local gains for up-to-5 link KUs with g–c vs. g–g internal conversion mode

KUs	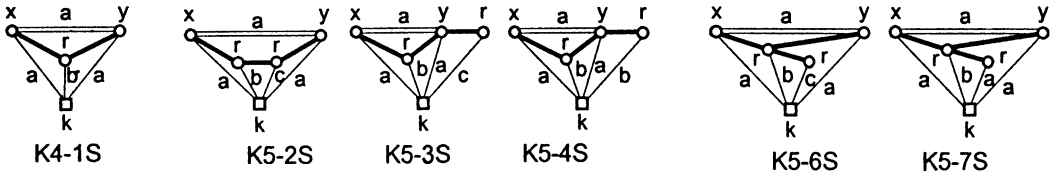
	K4-1S K5-2S K5-3S K5-4S K5-6S K5-7S
Local gain	$G(x,y;y,k)=\frac{\theta_{x,y}}{\theta_{y,k}}=(E_{y,x}-1);\ G(x,y;r,k)=\frac{\theta_{x,y}}{\theta_{r,k}}=(E_{y,x}-1)E_{r,y}$

Table 3
Local gains for up-to-5 link KUs with g–g vs. g–g internal conversion mode

KUs		
	K5-4D	K5-7D
Local gain	$G(x,q;y,p)=\frac{\theta_{x,q}}{\theta_{y,p}}=\frac{E_{p,x}-E_{p,q}}{E_{p,y}-1}$	$G(x,p;y,p)=\frac{\theta_{x,p}}{\theta_{y,p}}=\frac{E_{p,x}-1}{E_{p,y}-1}$

3.2. Local gain

The local gain of a KU is the gear ratio from local input to local output. According to the internal conversion mode, associated local gain can be derived as follows:

3.2.1. g–c vs. g–c type conversion

Since there is a unique carrier in each KU in Table 1, the kinematic relation between the two ends of the heavy-edged path can be derived by combining associated fundamental circuit equations as follows:

$$\theta_{y,k} = e_{x,x+1} \cdots e_{y-1,y}\theta_{x,k} = E_{x,y}\theta_{x,k} \tag{1}$$

where $\theta_{y,k}$ is the relative angular displacement between gear vertex y and the carrier k, $x+1$ represents the vertex on the right hand side of vertex x, $y-1$ represents the vertex on the left hand side of vertex y, $e_{x+1,x}$ is the gear ratio between vertices $x+1$ and x, and $E_{x,y}$ is the product of gear ratios on the heavy-edged path from x to y.

According to Eq. (1), we have:

Rule 1: The local gain of g–c vs. g–c type conversion can be expressed as:

$$G(y,k;x,k) = \frac{\theta_{y,k}}{\theta_{x,k}} = E_{x,y} \tag{2}$$

where x and y are gear vertices, and k is the unique carrier in the KU.

3.2.2. g–c vs. g–g type conversion

1. Conversion among coaxial vertices

For each KU in Table 2, the coaxial relation between two gear vertices, x and y, and the carrier k can be written as:

$$\theta_{x,k} = \theta_{x,k} - \theta_{y,k} \tag{3}$$

From Eqs. (2) and (3), we have:

Rule 2: The local gain of g–c vs. g–g type conversion among coaxial vertices can be expressed as:

$$G(x,k;y,k) = \frac{\theta_{x,k}}{\theta_{y,k}} = (E_{y,x} - 1) \tag{4}$$

where x and y are coaxial gear vertices, and k is the unique carrier.

2. Conversion including non-coaxial vertices

From Eq. (1), the kinematic relation between two gear vertices, r and y, and the carrier k can be derived as

$$\theta_{y,k} = E_{r,y}\theta_{r,k} \tag{5}$$

Combining Eqs. (4) and (5) yields

Rule 3: The local gain of g–c vs. g–g type conversion among non-coaxial vertices can be expressed as:

$$G(x,y;r,k)=\frac{\theta_{x,y}}{\theta_{r,k}}=(E_{y,x}-1)E_{r,y} \tag{6}$$

where x and y are coaxial gear vertices, r is another gear vertex which is connected to the carrier k with a thin edge with different axis label.

3.2.3. g–g vs. g–g type conversion

For the left hand side KU in Table 3, the local gains can be derived from Eq. (4) as

$$\theta_{x,q}=(E_{q,x}-1)\theta_{q,k} \tag{7a}$$

$$\theta_{y,q}=(E_{p,y}-1)\theta_{p,k} \tag{7b}$$

From Eq. (1), $\theta_{q,k}$ and $\theta_{p,k}$ can be related by

$$\theta_{p,k}=E_{q,p}\theta_{q,k} \tag{8}$$

By substituting Eq. (8) into Eq. (7b) and then eliminating $\theta_{q,k}$ in Eqs. (7a) and (7b), we have:

Rule 4: The local gain of g–g vs. g–g type conversion between two g–g type thin edges (x,q) and (y,p), which have different axis labels can be expressed as

$$G(x,q;y,p)=\frac{\theta_{x,q}}{\theta_{y,p}}=\frac{E_{p,x}-E_{p,q}}{E_{p,y}-1} \tag{9a}$$

For the right hand side KU in Table 3, the local gain can be derived along a similar procedure from Eqs. (7) to (9), and the following rule can be concluded:

Rule 5: The local gain of g–g vs. g–g type conversion between two coaxial g–g type thin edges (x,p) and (y,p) can be expressed as

$$G(x,p;y,p)=\frac{\theta_{x,p}}{\theta_{y,p}}=\frac{E_{p,x}-1}{E_{p,y}-1} \tag{9b}$$

Tables 1–3 show local gains of KUs with different internal conversion modes. With Tables 1–3, associated local gains of a KU can be formulated accordingly as the locations of local input and output are specified.

4. Global propagation

4.1. Common linkage

A common linkage is referred to as the interface among KUs and is composed of links and connecting thin edges shared by each other. From Figs. 2 and 3, two kinds of common linkages can be identified:

(1) *2-link-chain type*: This kind of common linkage exists between two KUs, and the relative angular displacement between links on the common linkage is used as the communicating medium between KUs. As shown in Fig. 1(d), KU_1 and KU_2 share a 2-link chain with vertices 1 and 5 on it.

(2) *Coaxial-triangle type*: This kind of common linkage exists among three KUs in which each pair of KUs shares a common vertex. As shown on the right hand side of Fig. 3, those thin edges forming the coaxial triangle are specially marked with short lines.

4.2. Kinematic propagation

For geared mechanisms with only one KU, kinematic propagation from input to output is completed in the same KU as shown in Fig. 4(a). Hence, the kinematic relation between input and output links can be described by *Rules 1–5*, which means that the global propagation is exactly equivalent to internal conversion.

For two KUs sharing a 2-link chain type common linkage, the output of a preceding KU is received directly by the succeeding KU as the input, the kinematic propagation path is shown as Fig. 4(b). Considering the mechanism in Fig. 1(d), $\theta_{3,5}$ and $\theta_{4,5}$ can be assigned as output and input, respectively. It can be observed that the lower KU labeled as KU_1 in which local input $\theta_{4,5}$ is transmitted to local output, $\theta_{1,5}$, on the common linkage through a g–c vs. g–c type conversion. Then, $\theta_{1,5}$ is received by the upper KU, which is labeled as KU_2, as local input from the common linkage and is subsequently converted into output, $\theta_{3,5}$ through a g–c vs. g–g type conversion. With the propagation through the common linkage, the motion is transmitted from KU_1 to KU_2.

As shown in Fig. 3, it is known that KUs around a coaxial-triangle type common linkage forms a 2-dof EGT. The coaxial relations result in a 2-input, 1-output interface among KUs, the kinematic propagation path is shown in Fig. 4(c). For instance, the graph in Fig. 3(a), which is composed of three K3-1 type KUs, can represent a 2-dof EGT by using $\theta_{1,4}$ and $\theta_{6,4}$ as input and $\theta_{3,5}$ as output. In the lower left KU, which is labeled as KU_1, local input $\theta_{1,4}$ is transmitted to local output $\theta_{2,4}$ on the common linkage. On the other hand, local input of the upper KU, which is

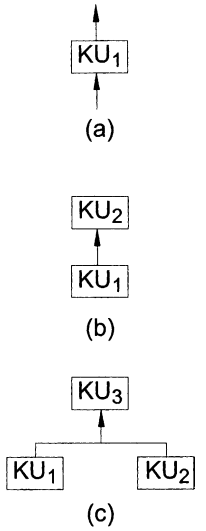

Fig. 4. Global propagation. (a) Single KU type, (b) 2-link chain type, (c) coaxial triangle type.

labeled as KU_2, $\theta_{6,4}$, is transmitted to local output $\theta_{5,4}$ on the common linkage. According to the coaxial condition, $\theta_{2,4}$ and $\theta_{5,4}$ are combined to form the resultant motion $\theta_{2,5}$ according to the following equation:

$$\theta_{2,5} = \theta_{2,4} + (-\theta_{5,4}) \tag{10}$$

The resultant motion is then received by the lower right KU, which is labeled as KUs, as local input and converted into output $\theta_{3,5}$. Hence, the propagation through a coaxial-triangle type common linkage needs two independent motions to initiate a resultant motion in the remaining KU around a coaxial triangle.

For geared mechanisms with multiple KUs, kinematic relations among input(s) and output(s) can be symbolically determined by virtue of a trace-back procedure from the KU with the global output. The procedure can be demonstrated as follows with the graph representation of EGT shown in Fig. 1(d) and the graph representation of EGT shown in Fig. 3(a) as examples.

Step 1: Express the global output in terms of local input of the associated KU.

The result can be generally expressed as:

$$\theta_{\text{out}} = {}^{\text{out}}[Kx - \#]_{\text{in}} \cdot \theta_{\text{in)L}} \tag{11}$$

where θ_{out} is the output, $\theta_{\text{in)L}}$ is the local input and ${}^{\text{out}}[Kx-\#]_{\text{in}}$ represents the local gain associated with the conversion from $\theta_{\text{in)L}}$ to θ_{out} in $Kx-\#$.

In Fig. 1(d), the output is located in KU_2 and its kinematic relation corresponding to Eq. (11) can be written as:

$$\theta_{3,5} = {}^{35}[K4 - 1S]_{15} \cdot \theta_{1,5} \tag{12}$$

In Fig. 3(a), the output is located in KU_3 and the relation corresponding to Eq. (11) can be written as:

$$\theta_{3,5} = {}^{35}[K3 - 1]_{25} \cdot \theta_{2,5} \tag{13}$$

where ${}^{35}[K3 - 1]_{25}$ is the local gain associated with the conversion from local input, $\theta_{2,5}$, to the local output, $\theta_{3,5}$ in KU_3 in the EGT in Fig. 3(a).

Step 2: Transform the local input in Eq. (11) into local output of preceding KU(s).

According to Fig. 4(b) and (c), the transformation can be determined by the following cases:

(a) For a 2-link-chain type common linkage, there is only one preceding KU, and the local output of the preceding KU is identical to the local input of its succeeding KU. Hence, there is no modification required for Eq. (11).
For the EGT in Fig. 1(d), the common linkage is a 2-link chain, and thus local input of KU_2, $\theta_{1,5}$, is equal to the local output of KU_1. Hence, Eq. (12) needs no modification.

(b) For a coaxial-triangle type common linkage, there are two preceding KUs from which two distinct local output merge into their succeeding KU. According to Eq. (10), Eq. (11) can be modified as:

$$\theta_{\text{out}} = {}^{\text{out}}[Kx - \#]_{\text{in}} \cdot (\theta_{\text{out})p1} + \theta_{\text{out})p2}) \tag{14}$$

where $\theta_{\text{out})p1}$ and $\theta_{\text{out})p2}$ are the two local output of preceding KUs.

For the EGT in Fig. 3(a), since KU_3 shares a coaxial-triangle type common linkage with preceding KUs, Eq. (13) can be rewritten according to Eqs. (10) and (14) as:

$$\theta_{3,5} = {}^{35}[K3 - 1]_{25} \cdot [\theta_{2,4} + (-\theta_{5,4})] \tag{15}$$

Step 3: Apply Eq. (11) to convert the local output(s) derived in *Step 2* into associated local input(s) and repeat *Steps 2* and *3* until all the local inputs are from KUs with input links. The final relation among global output and input can be generally expressed:

$$\theta_{\text{out}} = \sum_{m} \left(\prod {}^{\text{out}}[Kx - \#]_{\text{in}} \right) \cdot \theta_{\text{in})m} \tag{16}$$

where $(\prod^{\text{out}}[Kx - \#]_{\text{in}})$ represents the product of involved local gains from the input to output and $\theta_{\text{in})m}$ is the input contained in KU_m.

By applying Eq. (16) to the EGT in Fig. 1(d), Eq. (12) can be expanded as:

$$\theta_{3,5} = {}^{35}[K4 - 1S]_{15} \cdot {}^{15}[K3 - 1]_{45}\theta_{4,5} \tag{17}$$

where ${}^{15}[K3 - 1]_{45}$ is the local gain associated with the conversion from local input, $\theta_{4,5}$, to the local output, $\theta_{1,5}$ in KU_1 in Fig. 1(d).

By applying Eq. (16) to the EGT in Fig. 3(a), Eq. (15) can be expanded as:

$$\begin{aligned}\theta_{3,5} &= {}^{35}[K3 - 1]_{25} \cdot \{{}^{24}[K3 - 1]_{14} \cdot \theta_{1,4} - {}^{54}[K3 - 1]_{64} \cdot \theta_{6,4})\} \\ &= {}^{35} \cdot [K3 - 1]_{25} \cdot {}^{24}[K3 - 1]_{14} \cdot \theta_{1,4} - {}^{35}[K3 - 1]_{25} \cdot {}^{54}[K3 - 1]_{64} \cdot \theta_{6,4}\end{aligned} \tag{18}$$

where ${}^{24}[K3 - 1]_{14}$ is the local gain associated with the conversion from local input, $\theta_{1,4}$, to the local output, $\theta_{2,4}$ in KU_1 in Fig. 3(a), and ${}^{54}[K3 - 1]_{64}$ is the local gain associated with the conversion from local input, $\theta_{6,4}$, to the local output, $\theta_{4,5}$ in KU_2 in Fig. 3(a).

Eqs. (17) and (18) provide the global kinematic relation between the input and output as a polynomial in terms of local gains. The form of Eq. (17) implies that only one sequential kinematic propagating path exists in the EGT in Fig. 1(d) while multiple terms in Eq. (18) represents that the EGT in Fig. 3(a) contains two distinct propagating paths which merge at the coaxial-triangle type common linkage.

The local gains in Eqs. (17) and (18) can be substituted with the forms expressed in Tables 1–3. For the EGT in Fig. 1(d), ${}^{35}[K4 - 1S]_{15}$ can be determined by Table 2 as

$${}^{35}[K4 - 1S]_{15} = \frac{\theta_{3,5}}{\theta_{1,5}} = \left(-\frac{\theta_{1,5}}{\theta_{5,3}} \right)^{-1} = -[G(1,5;5,3)]^{-1} = \frac{-1}{(E_{5,1} - 1)} \tag{19}$$

${}^{15}[K3 - 1]_{45}$ can be determined from Table 1 as

$${}^{15}[K3 - 1]_{45} = \frac{\theta_{1,5}}{\theta_{4,5}} = G(1,5;4,5) = E_{4,1} \tag{20}$$

By substituting Eqs. (19) and (20) into Eq. (17), we have

$$\theta_{3,5} = \frac{E_{4,1}}{1 - E_{5,1}}\theta_{4,5} = \frac{e_{4,1}}{1 - e_{5,2}e_{2,1}}\theta_{4,5} \tag{21}$$

Similarly, the global kinematic relation of the EGT in Fig. 3(a) can be derived by converting Eq. (18) according to Table 1 as:

$$\theta_{3,5} = E_{2,3} \cdot E_{1,2} \cdot \theta_{1,4} - E_{2,3} \cdot E_{6,5} \cdot \theta_{6,4} = e_{2,3} \cdot [e_{1,2} \cdot \theta_{1,4} - e_{6,5} \cdot \theta_{6,4}] \tag{22}$$

5. An application to automatic transmission mechanisms

Fig. 5(a) shows the functional representation of a typical transmission mechanism, which is used as an example by Hsieh and Tsai [8]. From Fig. 5(a), it can be observed that the mechanism has three sets of sun-planetary-ring gear systems which corresponds to the three FGEs as shown in Fig. 5(b), in which the unlabeled vertex represents the housing. According to the connection between FGEs, a unique FGE diagram can be constructed for the mechanism, and then the overall gear ratio is determined by identifying the operation modes of associated FGEs [8].

In contrast to the three FGEs in Fig. 5(b), the mechanism has only two KUs as shown in Fig. 5(c) according to the concept of kinematic fractionation. The gear ratio analysis can be performed as follows with given location of ground, input and output links ([G, I, O]):

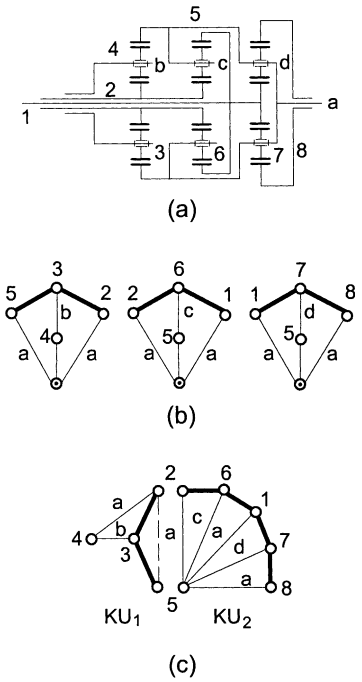

Fig. 5. A typical transmission mechanism. (a) Functional representation, (b) FGEs, (c) KUs.

1st gear with [G, I, O] = [5, 2, 8].

Since both the input and output links are in KU_2, the relation between the input and output is simply a g–c vs. g–c type internal conversion with the local gain as the overall gear ratio. From Table 1, the overall gear ratio at this operation mode is determined as:

$$\frac{\theta_{8,5}}{\theta_{2,5}} = E_{2,8} = e_{2,8} \tag{23}$$

2nd gear with [G, I, O] = [1, 2, 8].

The transmission from input, θ_{21}, to the output, θ_{81}, is a g–g vs. g–g type internal conversion in KU_2. From Table 3, the overall gear ratio at this operation mode is determined as:

$$\frac{\theta_{8,1}}{\theta_{2,1}} = \frac{E_{1,8} - 1}{E_{1,2} - 1} = \frac{e_{1,8} \cdot e_{7,8} - 1}{e_{1,6} \cdot e_{6,2} - 1} \tag{24}$$

3rd gear with [G, I, O] = [1, 4, 8].

In KU_2, the output θ_{81} can be expressed in terms of the local input, θ_{25}, as follows:

$$\theta_{8,1} = {}^{81}[\mathrm{KU}_2]_{25} \cdot \theta_{2,5} \tag{25}$$

where ${}^{81}[\mathrm{KU}_2]_{25}$ is the local gain associated with a g–c vs. g–g type conversion in KU_2.

Note that although KU_2 has six links, the connecting condition between local input and output is identical to those KUs in Table 2. Hence, ${}^{81}[\mathrm{KU}_2]_{25}$ can also be determined by fitting the expression in Table 2.

It can be observed that input θ_{41} involves both the two KUs in Fig. 5(c). According to the following coaxial condition, $\theta_{4,1}$ can be decomposed into two dependent terms which lie in different KUs:

$$\theta_{4,1} = \theta_{4,2} + \theta_{2,1} \tag{26}$$

Eq. (26) can be related to the local output of KU_1 as

$$\theta_{4,1} = \{{}^{42}[K4 - 1S]_{25} + {}^{21}[K4 - 1S]_{25}\} \cdot \theta_{2,5} \tag{27}$$

where both terms of local gains in Eq. (27) are associated with the g–c vs. g–g type conversion in KU-$4 - 1S$.

Re-arranging Eq. (27) yields

$$\theta_{2,5} = \{{}^{42}[K4 - 1S]_{25} + {}^{21}[K4 - 1S]_{25}\}^{-1} \cdot \theta_{4,1} \tag{28}$$

By substituting Eq. (28) into Eq. (25), the overall gear ratio at the third gear are determined as

$$\frac{\theta_{8,1}}{\theta_{4,1}} = {}^{81}[\mathrm{KU}_2]_{25} \cdot \{{}^{42}[K4 - 1S]_{25} + {}^{21}[K4 - 1S]_{25}\}^{-1} \tag{29}$$

where the local gains can be further expanded in terms of gear ratios according to Table 2.

It can be seen that the concept of FGEs are obtained from structural aspects rather than from kinematic characteristics, over decomposition may be occurred. As shown in Fig. 5(b), the second and third FGEs should be considered as a single KU since they share a carrier. Hence, it is

believed that KUs represent more direct and efficient modules than FGEs in conducting kinematic analysis of geared mechanisms.

6. Conclusion

The concept of kinematic fractionation is introduced to identify the kinematic modules in geared mechanisms. The concept of kinematic fractionation exposes the kinematic propagation in the mechanism and facilitates the determination of global kinematic relation between input and output links. Admissible internal conversion modes and associated local gains are determined for KUs with up to five links. According to the internal conversion mode in each KU, input and output can be correlated by sequential substitution along the global kinematic propagating path(s). It is believed that the proposed approach provides much kinematic insight into the interactions in geared mechanisms.

Acknowledgment

The financial support of this work by the National Science Council of the Republic of China under the Grant NSC 90-2212-E-002-166 is gratefully acknowledged.

References

[1] G.H. Martin, Kinematics and Dynamics of Machines, second ed., McGraw-Hill, NY, 1982.
[2] A.G. Erdman, G.N. SandorMechanism Design: Analysis and Synthesis, vol. 1, Prentice Hall, Eaglewood Cliffs, NJ, 1991.
[3] K.J. Waldron, G.L. Kinzel, Kinematics, Dynamics, and Design of Machinery, John Wiley and Sons, New York, 1999.
[4] F. Freudenstein, An application of Boolean algebra to the motion of epicyclic drives, ASME Journal of Engineering for Industry 93 (B) (1971) 176–182.
[5] F. Freudenstein, A.T. Yang, Kinematics and statics of a coupled epicyclic spur-gear train, Mechanism and Machine Theory 7 (1972) 263–275.
[6] L.W. Tsai, The kinematics of spatial robotic bevel-gear trains, IEEE Journal of Robotics and Automation 4 (2) (1988) 150–155.
[7] G. Chatterjee, L.W. Tsai, Computer-aided sketching of epicyclic-type automatic transmission of gear trains, ASME Journal of Mechanical Design 118 (1996) 405–411.
[8] H.I. Hsieh, L.W. Tsai, Kinematic analysis of epicyclic type transmission mechanisms using the concept of fundamental geared entities, ASME Journal of Mechanical Design 118 (1996) 294–299.
[9] D.Z. Chen, S.C. Shiue, Topological synthesis of geared robotic mechanism, ASME Journal of Mechanical Design 120 (1998) 230–239.
[10] D.Z. Chen, Kinematic analysis of geared robot manipulators by the concept of structural decomposition, Mechanism and Machine Theory 33 (7) (1998) 975–986.
[11] C.P. Liu, D.Z. Chen, On the embedded kinematic fractionation of epicyclic gear trains, ASME Journal of Mechanical Design 122 (2000) 479–483.
[12] C.P. Liu, D.Z. Chen, On the application of kinematic units to the topological analysis of geared mechanisms, ASME Journal of Mechanical Design 123 (2000) 240–246.

[13] L.W. Tsai, C.C. Lin, The creation of non-fractionated two-degree-of-freedom epicyclic gear trains, ASME Journal of Mechanisms, Transmissions, and Automation in Design 111 (1989) 524–529.
[14] L.W. Tsai, An application of the linkage characteristic polynomial to the topological synthesis of epicyclic gear trains, ASME Journal of Mechanisms, Transmissions, and Automation in Design 109 (3) (1987) 329–336.